Accepted Manuscript

A novel nucleic acid fluorescent sensing platform based on nanostructured films of intrinsically conducting polymers

Graciela C. Pedro, Filipe D.S. Gorza, Romário J. da Silva, Kamila T.O. do Nascimento, Juan C. Medina-Llamas, Alicia E. Chávez-Guajardo, José J. Alcaraz-Espinoza, Celso P. de Melo

PII: S0003-2670(18)31212-1

DOI: 10.1016/j.aca.2018.10.010

Reference: ACA 236316

To appear in: *Analytica Chimica Acta*

Received Date: 25 June 2018

Revised Date: 5 October 2018

Accepted Date: 8 October 2018

Please cite this article as: G.C. Pedro, F.D.S. Gorza, R.J. da Silva, K.T.O. do Nascimento, J.C. Medina-Llamas, A.E. Chávez-Guajardo, J.J. Alcaraz-Espinoza, C.P. de Melo, A novel nucleic acid fluorescent sensing platform based on nanostructured films of intrinsically conducting polymers, *Analytica Chimica Acta* (2018), doi: https://doi.org/10.1016/j.aca.2018.10.010.

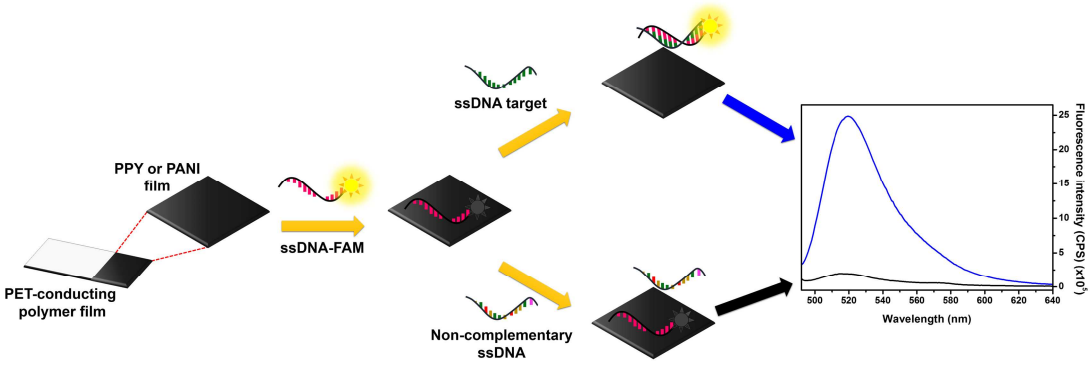

A novel nucleic acid fluorescent sensing platform based on nanostructured films of intrinsically conducting polymers

Graciela C. Pedro [a], Filipe D. S. Gorza [a], Romário J. da Silva [a], Kamila T. O. do Nascimento [a], Juan C. Medina-Llamas [b], Alicia E. Chávez-Guajardo [c], José J. Alcaraz-Espinoza [d], Celso P. de Melo [a, d *]

[a] *Pós-Graduação em Ciência de Materiais, Universidade Federal de Pernambuco, 50670-901 Recife, PE, Brazil*

[b] *Centro de Estudios Científicos y Tecnológicos No. 18, Instituto Politécnico Nacional, 98160, Zacatecas, Zac, Mexico*

[c] *Unidad Académica de Ciencias de la Tierra, Universidad Autónoma de Zacatecas, 98058 Zacatecas, Zac, Mexico*

[d] *Departamento de Física, Universidade Federal de Pernambuco, 50670-901 Recife, PE, Brazil*

*Corresponding author:

Prof. Celso Pinto de Melo

E-mail: celso@df.ufpe.br

Tel.: +55 81 21267612; fax: +55 81 32717603.

ABSTRACT

When fluorophores attach to nanostructured films of intrinsically conducting polymers (ICPs), a quenching of their fluorescence may occur. We have exploited these characteristics for the development of polymeric films that can be used in a simple and efficient molecular diagnosis protocol based on the selective detection of nucleic acids. Our procedure rests on the fact that the fluorescence of 6-carboxyfluorescein-labeled single-stranded DNA (FAM-ssDNA) probes is quenched upon their immobilization on nanostructured ICP – polypyrrole (PPY) and polyaniline (PANI) – films deposited on polyethylene terephthalate (PET) substrates. Hybridization occurs whenever a sample with the complementary sequence is brought in contact with the immobilized probe, with the newly formed ds-DNA chains detaching from the flexible polymeric film and causing the restoration of the fluorescence. This sensing system exhibits a low background signal that depends on both the thickness and hydrophobicity of the films. As a model system, we used a FAM-ssDNA probe specific for the *Leishmania infantum* parasite. The results confirm this procedure as a simple, fast and highly sensitive scheme for the recognition of the target DNA, with a detection limit of the 1.1 nM and 1.3 nM for the PPY/PET and PANI/PET films, respectively. In addition, this biosensor has excellent stability and exhibits a good and reproducible performance even when used for the direct detection of ssDNA in relatively complex biological samples.

Keywords: nanostructured films; conducting polymers; molecular diagnosis; fluorescent detection; test strips.

1. INTRODUCTION

In the last decades, exhaustive research has been dedicated to the development of simple, fast, and low-cost portable biosensors for the rapid detection of deoxyribonucleic acid (DNA) chains. Simple and fast DNA detection can be considered as a key step for point-of-care applications related to the prompt diagnosis of infectious or genetic diseases (a feature of special impact both for prevention and a possible early treatment), for inexpensive environmental monitoring and in the rapid identification of pathogens in the food industry [1, 2]. At present, there is a vast number of well-established methods for the highly specific detection of DNA hybridization based on different transduction principles (such as exploiting convenient optical [3, 4], electrochemical [5, 6], impedimetric [7, 8], spectrometric [9], gravimetric [10] properties, among others). However, some of these procedures tend to be both time-consuming and expensive, requiring complicated or specialized equipment, characteristics that represent practical impediments to their more widespread implementation in point-of-care applications [11].

Currently, laboratorial gold standard protocols for nucleic acid detection are based on the polymerase chain reaction (PCR) technique. This technique involves the sample amplification and requires a careful design of the synthetic oligonucleotides to be used as initiators in accurate temperature-controlled cycles to obtain sensitivities in the fM (10^{-15} M) range with the high specificity for discriminating even a single mismatched base. However, the high cost of the corresponding instrumentation, the time required to complete the analysis and the need for contamination-free environments (plus the requirement of specialized professionals to perform the tests) are practical obstacles to a more widespread use of this technology in regular diagnostics for on-site detection in primary point-of-care [2, 10]. Therefore, there is a need for the development of inexpensive and simple molecular diagnostic procedures that would not necessarily replace PCR analyses, but rather complement them as efficient pre-screening methods.

Lately, sensitive and more specific methods based in the use of nanomaterials, which are also faster and cost-effective, have been introduced in the field of molecular biorecognition. An important example of this is the notable development of nanostructured fluorescent sensors [12-15] that present several competitive advantages, such as simple operation requirements, high sensitivity, possibility of automation and the capability of *in situ* imaging [16, 17].

An interesting novel application of nanomaterials in sensors is their use as nanoquenchers in fluorescent DNA assays. In this type of test, the nanostructure mainly interacts with the fluorophore of a labeled DNA probe through electron transfer processes that result in the quenching of the emission. Restoration of the fluorescence would only be achieved in the presence of a target DNA complementary to the original DNA probe, when the probe-target hybridization would cause desorption of the labeled probe into the supernatant. Nanostructures of this type have received considerable attention because of their unique optical, catalytic and electronic properties, which allow an efficient quenching of the fluorophore emission for a wide range of frequencies [18]. To date, various types of nanostructures, such as carbon nanotubes [19], graphene oxide [12, 18], Au [20], Ag [11, 21] and ceria [22] nanoparticles, quantum dots [16], metal-organic structures [13, 23], transition metal nanosheets [24, 25] and conductive polymers – such as poly(3,4-ethylenedioxythiophene) (PEDOT) nanoparticles [26], polypyrrole (PPY) nanospheres [27], polyaniline (PANI) nanofibers [28], have been reported as effective fluorescence quenchers for detecting nucleic acid sequences. However, it would be convenient to simplify the corresponding operational procedures, and a convenient manner of achieving this is by immobilizing these nanostructures on flexible substrates that could be integrated in portable devices, allowing more extensive applications. Alternatively, the immobilized nanostructures could be previously functionalized with the probe of interest and then used as fluorescence test strips – a procedure that would reduce the time required to perform a diagnosis assay.

In the development of new sensing platforms, flexible polymers such as polyethylene terephthalate (PET) appear as convenient substrates to be considered. In that regard, PET offers several comparative advantages, such as enhanced and adjustable physical-chemical properties, heat conductivity and thermal stability at temperatures up to 180 °C [29]. Differently from paper, plastics do not experience sample retention, an important feature that enables a more precise delivery of materials in the sensing process. Self-standing nanostructured films involve simple preparation procedures and can be conveniently handled and recovered after use, important comparative advantages relative to conventional detection platforms based in other nanomaterials, such as particulate dispersion or colloids. These characteristics contribute to a smaller background signal, due to the minimization of the presence of contaminants that could confound the interpretation of the results. Another important aspect to consider is that agglomeration (a common nuisance when working with some nanostructures) is minimized when the adsorbent material is deposited in the form of films.

The purpose of the present work is the development of a film platform composed by nanostructured intrinsic conducting polymers (ICPs) deposited on PET foils that could be used as an efficient biosensing system based on the quenching of fluorescence of specific DNA probes. We selected ICPs due to their peculiar electronic, chemical, physical and optical properties and the possibility of forming nanostructures by the proper tweaking of the synthesis conditions. We decided to focus our work on PANI and PPY, as they present advantages over other ICPs in terms of simplicity of synthesis, richer doping-dedoping chemistry, low-cost, and excellent environmental stability [30, 31]. For us, the most important aspect to consider is that these ICPs not only interact with the fluorophore but also form complex structures with the DNA molecules, a factor that contributes to an efficient adsorption of the DNA probe [27, 28, 32].

In this work, we used as a model system biosensing strips consisting of nanostructured ICP/PET films for the detection of oligonucleotide sequences characteristic of the *Leishmania*

infantum parasite, a species that causes leishmaniasis – a neglected disease of great incidence in tropical countries. We carried out a detailed study considering different physical-chemical parameters of the films, such as their thickness, the probe-target interaction time, and the quenching efficiency. We believe that this approach may contribute to a better understanding of the characteristics of nanostructured films when used as quenching agents in molecular diagnostic tests by fluorescence, in an innovative procedure that bears a promising potential for applications in point-of-care devices. To the best of our knowledge, the use of nanostructured films as quenchers for the fluorescence detection of nucleic acids has not yet been duly investigated.

2. EXPERIMENTAL

2.1. Materials

Transparent PET foils with a thickness of 75 µm were obtained from Filiperson (Brazil). Aniline, magnesium chloride ($MgCl_2$), hydrochloric acid ($HCl_{(aq)}$), and iron (III) chloride hexahydrate ($FeCl_3.6H_2O$) were supplied by the Brazilian companies Nuclear, Vetec-Química Fina, Química Moderna and Dinâmica, respectively. Pyrrole, ammonium persulfate (APS) and tris(hydroxymethyl)aminomethane (TRIS) were purchased from Sigma-Aldrich (USA). The oligonucleotide sequences used in this study, which were synthesized and purified by ThermoFisher Scientific (USA), are listed in Table 1. All reagents were of analytical grade and used as received without further purification, except for aniline and pyrrole, which were distilled under reduced pressure prior to use. In all experiments, we used ultra-high purity water obtained from a Synergy Purification System (Millipore, USA).

Table 1. Oligonucleotide sequences used in this work (mismatch underlined).

Name	Oligonucleotide sequence
FAM-ssDNA Linf.1-23F – *Leishmania*	5'- FAM-TCC CAA ACT TTT CTG GTC CT -3'
Complementary target DNA (T_0)	5'- AGG ACC AGA AAA GTT TGG GA -3'

Single-base-mismatched target DNA (T_1)	5'- AGG ACC AGA **C**AA GTT TGG GA -3'
Two-base-mismatched target DNA (T_2)	5'- AGG ACC AGA **C**A**C** GTT TGG GA -3'
Non-complementary target DNA (ncDNA)	5'- GAA ACT GGG GGT TGG TGT AA -3'

2.2. Preparation of PET-polyaniline and PET-polypyrrole films

Initially, square foils of PET with 32 mm sides were cleaned with detergent and rinsed with deionized water, and then sonicated in isopropanol for 15 min. Then, 22 mm x 32 mm rectangular masks were prepared using scotch tape pasted to both sides of the freshly cleaned PET substrates. The deposition of PPY and PANI on PET foils was carried by an *in situ* chemical polymerization.

2.2.1. *In situ* chemical polymerization of PPY

The PPY chains were deposited according to the following methodology: initially, 1 mmol of pyrrole was diluted in 49 mL of deionized water and added into a 250 mL beaker, where the masked PET foil was vertically placed to allow the growth of the polymeric film on both sides of the substrate. Then, 750 µL of a 1.0 M $FeCl_3$ aqueous solution was slowly added to initiate the polymerization, which we allowed to proceed during 12 h at low temperature (~ 5 ºC) and under constant stirring on an orbital shaker. Finally, the films obtained were washed several times with deionized water, dried with a stream of dry compressed air, and cut in 8 mm wide strips.

2.2.2. *In situ* chemical polymerization of PANI

The PANI films were obtained by implementing slight changes to the above procedure. The synthesis was carried out in a 1 M aqueous solution of $HCl_{(aq)}$, by adding aniline (0.66 mmol) and APS (0.33 mmol) as oxidant. Films of PPY or PANI with different thicknesses were obtained by subjecting the PET foils to 1, 2 or 3 successive polymerization cycles. In Scheme 1a, we present a pictorial representation of the preparation process of the PPY and PANI films.

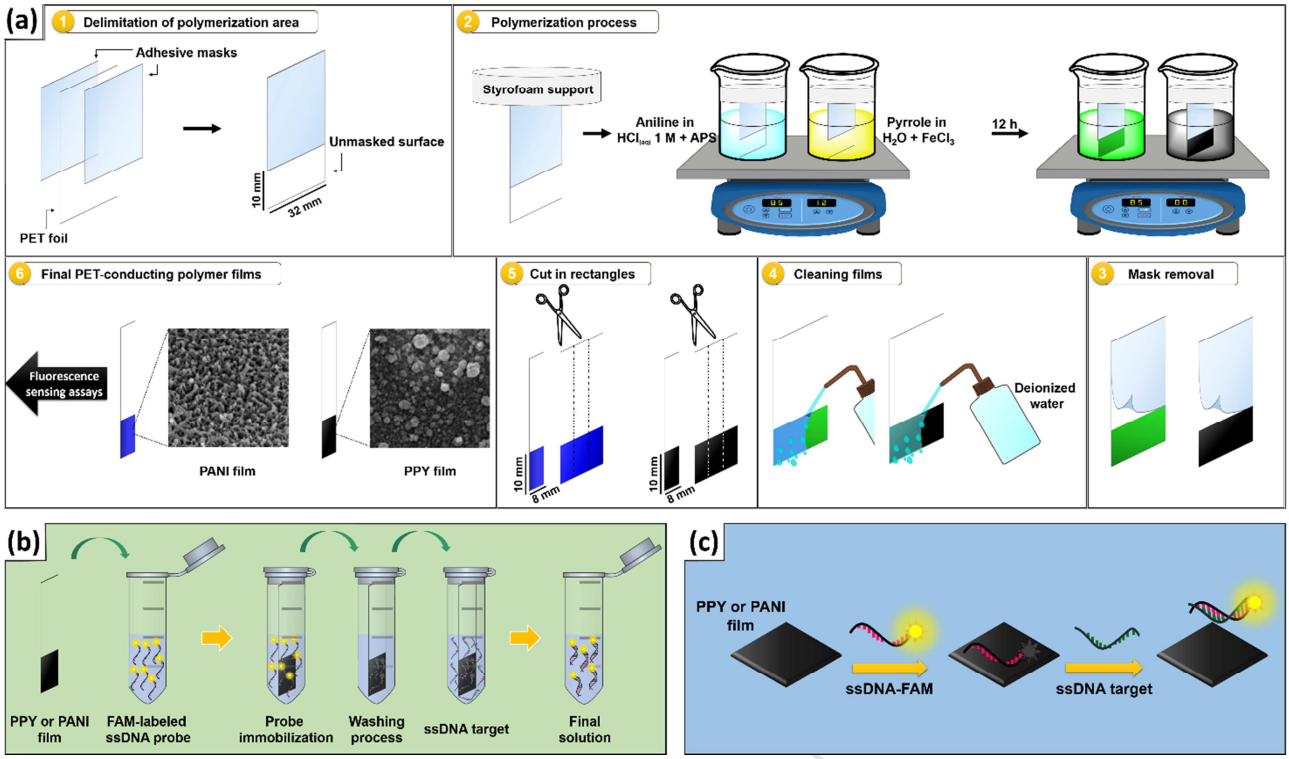

Scheme 1. Schematic representations of: (a) steps involved in the preparation of PANI and PPY films, (b) method used to perform the fluorescence sensing assays, and (c) mechanism of fluorescence detection of nucleic acids by use of nanostructured ICP/PET films as sensing platforms.

2.3. Characterization methods

The morphological characteristics of the PPY and PANI films were assessed by use of a MIRA3 microscope (TESCAN, CZ). The thickness of the films was measured using an Alpha 300 atomic force microscope (Witec, Germany). Attenuated total reflectance Fourier transform infrared (ATR-FTIR) spectra in the 2000–630 cm^{-1} range were recorded using an IRTracer-100 spectrometer (Shimadzu, Japan). A ZnSe crystal was used in an ATR cell, with 4 cm^{-1} resolution, with an average of 64 scans. The hydrophobic/hydrophilic character of the films was analyzed by use of a CAM 100 contact angle meter instrument (KSV, Finland). To confirm the composition of the material and identify the oxidation state of the incorporated PANI and PPY, UV-vis spectra of the films were collected by using an UV-2600 spectrophotometer (Shimadzu, Japan). The concentration of the stock solutions of DNA was determined by use of an UV-vis NanoDrop 2000 spectrophotometer (Thermo-Scientific, USA). All fluorescence measurements were performed using a FluoroLog-3

spectrofluorimeter (Horiba, USA). The excitation wavelength was fixed at 480 nm, with the emission spectra recorded over the 490-650 nm range.

2.4. Fluorescence sensing assays

In Scheme 1b we depict the method used to perform the fluorescence sensing assays. For the fluorescence quenching experiment, the PPY and PANI films were placed to interact with 1 mL of a 75 nM FAM-labeled ssDNA probe diluted in Tris-HCl buffer (pH 7.4) in presence of 10 mM $MgCl_2$ for 180 min, and under constant stirring. Then, using tweezers, the films were removed from the FAM-ssDNA solution and subjected to a cleaning process that consisted of three consecutive 30 min washings using 1 mL of Tris-HCl buffer (pH 7.4) in presence of 10 mM $MgCl_2$. The implementation of a washing step prior to the hybridization experiments is an important precaution to assure that only those immobilized probes firmly attached to the surface of PPY or PANI remain on the substrate. To perform the hybridization experiments, the FAM-ssDNA/PPY and FAM-ssDNA/PANI systems were placed in contact with different concentrations – in the (1-600) nM range – of the complementary target DNA for 60 min at room temperature (~23 °C). Finally, the film was removed from the solution containing the complementary target DNA and the fluorescence intensity of the supernatant measured. All experiments were performed under constant stirring (300 rpm) in an orbital shaker. We chose to work with 75 nM probe solutions after a preliminary investigation had shown that at this concentration all available adsorption sites in both types of films were fully saturated. All results shown for the sensing experiments correspond to the average of measurements made on five different films.

3. RESULTS AND DISCUSSION

3.1. Characterization of PPY and PANI films

We examined the composition of the PET foils and of the PANI and PPY films by using FTIR spectroscopy (Fig. 1a). As one can observe, the PET spectrum (curve i) exhibits four major peaks: one at 1714 cm^{-1} associated with the terephthalic acid C=O ester group, two others at 1248 cm^{-1} and 1099 cm^{-1}, which are characteristic of polyethylene terephthalate and can be assigned to the C-C-O and the O-C-C asymmetric stretching, respectively, and a 722 cm^{-1} peak attributed to the C-H wagging vibrations in the aromatic structures [33]. All characteristic bands are present in the spectrum of the PPY films (curve ii): the bands at 1548 cm^{-1} and 1452 cm^{-1} correspond to the C=C and C-N stretching vibrations, respectively, whereas the bands at 1300 cm^{-1} and 1163 cm^{-1} are associated with C-H in-plane vibrations, and the bands at 887 cm^{-1} and 777 cm^{-1} are assigned to C-H out-of-plane vibrations [34-36]. In the case of PANI films (curve iii), the main bands that are observed at 1573 cm^{-1} and 1496 cm^{-1} can be assigned to the C=C stretching deformation in the quinoid and benzenoid rings, respectively. Finally, the bands at 1300 cm^{-1} and 817 cm^{-1} are correlated to the C-N stretching vibrations and C-H out-of-plane deformations in the benzenoid rings, respectively [36-38].

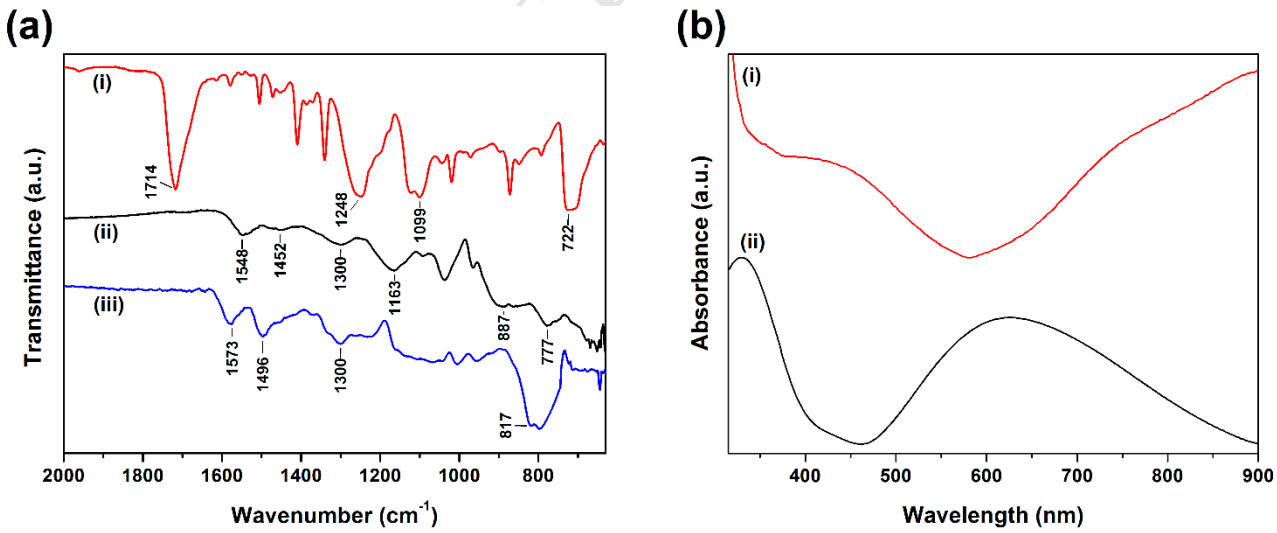

Figure 1. (a) FTIR-ATR spectra of (i) PET foil and (ii) PPY and (iii) PANI films. (b) UV-vis spectra of (i) PPY and (ii) PANI films.

We investigated the oxidation state of the conducting polymers films (Fig. 1b) by analyzing the corresponding UV-vis spectrum. Before making these measurements, the films were washed with an aqueous solution of pH 6.0 and then dried. In curve i (PPY spectrum) of Fig. 1b, the absorption band observed at 450 nm can be assigned to the $\pi - \pi^*$ transition and, as usual, the broad one above 600 nm is associated to the presence of bipolarons, the typical charge carriers of doped PPY [39, 40]. Curve ii (PANI spectrum) exhibits two bands at 330 nm and 620 nm, which are characteristic of the emeraldine base, the undoped form of PANI. The first one is associated with the $\pi - \pi^*$ transition of the benzene rings, while the latter is assigned to the molecular exciton transition [41, 42]. These differences observed in the oxidation state of the PPY and PANI films occur because changes in the pH of the medium do not affect the doped state of PPY as much as that of PANI. Thus, positive charges will remain present in the PPY chains even at pH 6.0.

High-magnification SEM images of the PET foil (Fig. S1 in the Supporting Information) and of the PANI and PPY films (Fig. 2) were obtained. In Fig. S1 one can observe that the surface of the pristine PET foil is smooth and uniform, presenting no evident roughness. Both the PANI and PPY films deposited atop the PET foils were observed to be homogeneous (Fig. 2). As shown in Fig. 2a [2d], after the first polymerization cycle a film exhibiting nanofibers [nanograins] and with a thickness of approximately (213 ± 9) nm [(280 ± 16) nm] was obtained in the case of PANI [PPY]. However, with the second and third polymerization cycles, the thickness of these PANI [PPY] nm films increases to (592 ± 22) nm [(452 ± 32) nm] and (1036 ± 20) nm [(967 ± 37) nm], respectively, with the roughness becoming more pronounced and with a larger presence of nanostructures that cover the entire PET surface (Figs. 2b-2c and 2e-2f). A general overview of the surface structure of the corresponding films can be found in the low-magnification SEM images presented as insets in Figs. 2a-2f. The average values of the measured roughness of the ICP/PET films are shown in Table S1 (Supporting Information).

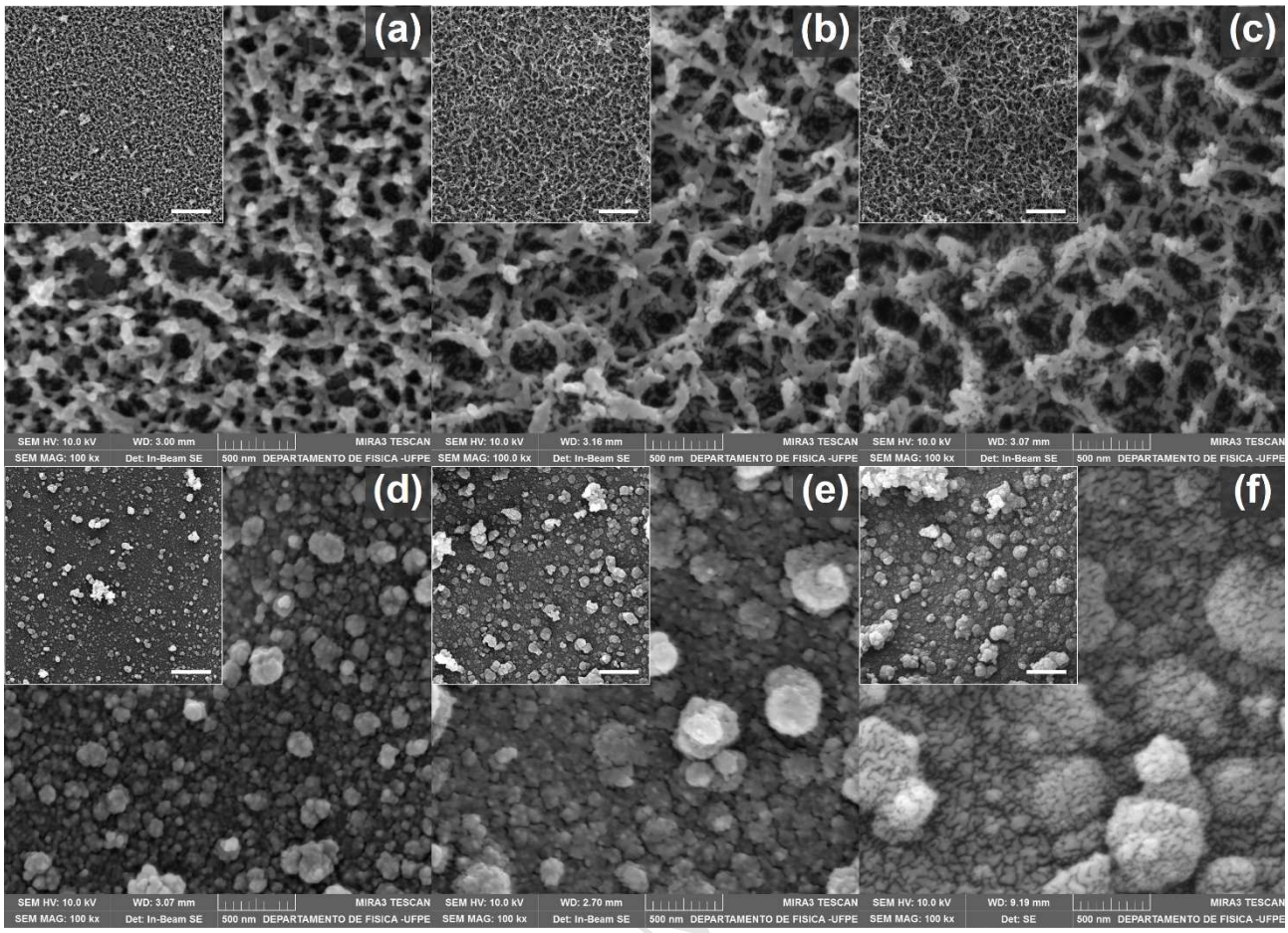

Figure 2. SEM images of PANI (a, b and c) and PPY (d, e and f) films prepared using 1, 2 and 3 polymerization cycles, respectively. SEM images at low magnification (the scale bar refers to 2 μm) are shown in the corresponding insets.

In fact, the procedure adopted for confining the growth of the PANI nanostructures mainly on the PET surface (and not in the bulk solution) relies on using both a low concentration of reagents and a low polymerization temperature, and it is based on a mechanism that has been already discussed in the literature regarding the polymerization of aniline on solid substrates [43-45]. Upon these preparation conditions, the time required for inducing the polymerization is long enough for the nucleation sites to arise first on the surface of the solid substrates and not directly into the solution. The generated nucleation sites minimize the interfacial energy barrier, and thus the freshly established aniline oligomers anchor close to these sites, stimulating the growth of new PANI chains. Since this process occurs along the entire solid surface in contact with the reaction

solution, formation of a PANI film is favored; for steric reasons, the growth of the deposited polymer is oriented along directions perpendicular to the available surfaces. On the other hand, the deposition of PPY on top of the substrate must occur through precipitation [46]: the radical cations – resulting from the oxidation of the pyrrole monomer – combine, forming insoluble oligomers that spontaneously deposit as a thin layer on the surface of the solid substrate immersed in the polymerization solution [47].

3.2. Use of PANI and PPY films for the detection of biomolecular interactions

As illustrated in Scheme 1c, the procedure for DNA detection based on the use of PPY and PANI films as a sensing platform involves first the immobilization of fluorescently labeled single-stranded DNA (FAM-ssDNA) chains on the surface of the polymeric film, leading to the quenching of the luminescence signal. Subsequently, when the FAM-ssDNA/ICP film system is put in contact with the target DNA solution, the specific hybridization of the probe with its complementary target causes the release of the FAM-ssDNA from the surface of the films. With this, double-stranded DNA (dsDNA) chains are formed and, as a result, the fluorescence is recovered.

To assess the efficiency of this strategy, we choose to use as model system probe molecules comprised by FAM-labeled oligonucleotide sequences associated with the *Leishmania infantum* parasite. In Fig. 3, we present the fluorescence emission spectra of the FAM-ssDNA probe (75 nM) under different conditions. In curve a, it is possible to observe that the initial (i.e., as prepared) probe solution exhibits a strong fluorescence emission due to the fluorescein dye coupled to the probe structure, whereas the intensity of the fluorescence emission decreases 57% [84%] after a 180 min interaction with PANI (curve b) [PPY (curve c)] films. This is in fact an indication that these films strongly adsorb the FAM-ssDNA probe. With the probe firmly immobilized, each one of the two FAM-ssDNA/ICP film systems was immersed into a solution of the target DNA (either a complementary (T_0) or a non-complementary (ncDNA) single chain). When the intensities of the

recovered fluorescence of the T_0 and ncDNA supernatants were compared, the largest response was indeed found for the case of the complementary target DNA (inset of Fig. 3), confirming that under this protocol both the PANI and the PPY films are effective for probing biomolecular interactions.

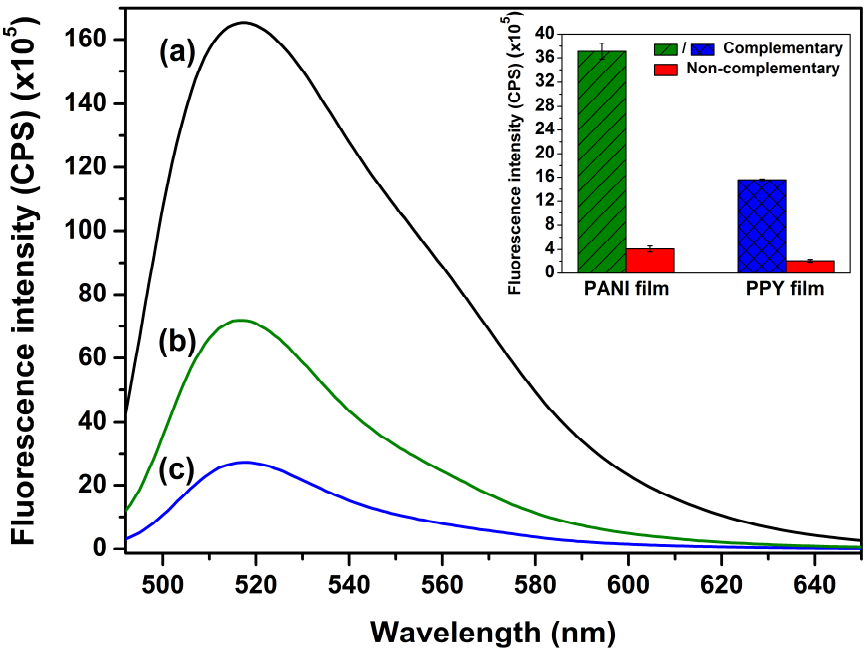

Figure 3. Fluorescence emission spectra of FAM-ssDNA solution (75 nM) under different conditions: before (a) and after interaction with single polymerization PANI (b) and (c) PPY films. Inset: intensity of the fluorescence after interaction of FAM-ssDNA/PPY and FAM-ssDNA/PANI systems with complementary and non-complementary target ssDNA (50 nM).

This sensing mechanism can be better understood if one considers the different affinities of single and double stranded DNA chains towards the PANI and PPY surfaces. As shown in Fig. S2, while only a slight change in the fluorescence intensity is observed after a FAM-dsDNA is placed in contact with the PPY and PANI films, a large decrease occurs when either of these films interact with a FAM-ssDNA solution. This indicates that the affinity of the dsDNA towards the active sites on the surface of the ICP films is much weaker than that of the ssDNA chains.

Both PANI and PPY exhibit a π-rich conjugated structure. Hence, during the immobilization of the FAM-ssDNA probes, strong hydrophobic π-π interactions of the nitrogenous bases of ssDNA molecules with the aromatic rings of the polymers are favored [43, 48]. In addition, hydrogen bonds

between primary amines of the ssDNA molecules and secondary amines of the PANI can be formed, as well as electrostatic interactions, are established between the positive charge of the amine group of the PPY and the negative charges of the phosphate groups present in the molecules of DNA. After the FAM-ssDNA molecules are immobilized, the quenching of the FAM fluorescence occurs via the photoinduced electron transfer between the excited fluorophore and the PANI or PPY chains, which is favored by the now closer proximity between the emitter and the absorber [28].

Hybridization occurs when the FAM-ssDNA/ICP films are exposed to a solution of complementary ssDNA, and dsDNA chains are formed after the probe undergo a conformational change and detach from the surface of the film. The nitrogenous bases of FAM-ssDNA are now hidden in the rigid helical dsDNA structure and only the negatively charged phosphate groups remain exposed. As a result, the fluorescence of the fluorophore is recovered in the liquid phase.

3.3. Optimization of the *Leishmania infantum* DNA detection

To establish the best conditions for using the PANI and PPY substrates as fluorescence sensing platforms of specific sequences of DNA, we varied some preparation parameters, such as i) the film thickness (controlled by the number of implemented polymerization cycles), ii) the time allowed for the immobilization of the FAM-marked probe, and iii) the total time allotted for the hybridization step, and then examined the corresponding effects upon the sensitiveness of the sensor. For this, we initially monitored the quenching of the fluorescence signal and its subsequent recovery as a function of the film thickness. In Figs. S3a and S3c one can observe that the fluorescence of the initial FAM-ssDNA solution decreases drastically after the labelled single DNA chains interact with a single-layer film of either PPY or PANI, and that a slighter increase in the amount of further adsorbed probes occurs for the ICP films prepared with 2 and 3 polymerization cycles.

As for the recovery of fluorescence intensity, a distinct behavior was observed when we allowed FAM-ssDNA/ICP films of different thicknesses interact with the complementary target DNA (Figs. S3b and S3d). A larger fluorescence recovery was obtained when a single-layer ICP film was used, a result that we attribute to the fact that thicker films (i.e. those obtained after 2 or 3 polymerization cycles) have a larger number of active sites available for adsorption of ssDNA chains. Under these conditions, many of these sites can interact with the dissolved target DNA chains, immobilizing them on the surface of the film. This competing process will reduce the number of dsDNA in the supernatant, thus diminishing the degree of recovery of fluorescence. As a check of this hypothesis, the adsorption on thicker (2 and 3 layer) films was monitored as a function of time (see Fig. S4 in the Supporting Information).

In Fig. S3, it is also possible to observe that the PPY films adsorb more of the FAM-ssDNA probe than the PANI based substrates. However, as shown in Figs. S3b and S3d, a lower fluorescence recovery was obtained when the FAM-ssDNA/PPY system was exposed to the solution of complementary DNA target. This probably occurs because any nonspecific interaction between the FAM-ssDNA and the target DNA is minimized due to the stronger adsorption of the probe on the surface of PPY films. In fact, the data of Fig. S5 reveal that the surface of the PPY films is more hydrophobic than that of the PANI substrates (the respective contact angles are $(98 \pm 1)^{o}$ and $(58 \pm 4)^{o}$). Therefore, hydrophobic π-π interactions between the FAM-ssDNA nucleobases and the aromatic rings in the polymer chains are more favored in the PPY case. Since for both cases the best sensing results were obtained when the ICP is deposited as a single-layer, all subsequent studies were carried out using the films prepared with just one polymerization cycle.

It is also interesting to note that when the FAM-ssDNA/PANI films are exposed to a blank sample (a Tris-HCl (pH 7.4) + 10 mM $MgCl_2$ solution), the background fluorescence signal increases with the number of the deposited polymeric layers, contrary to what one observes when the PPY-based substrates are used (Fig. S6). As discussed before, due to its lower hydrophobicity

PANI exhibits a lower affinity towards the FAM-ssDNA, so an increase on the number of polymeric layers would favor the dissolution of the immobilized probes, leading to an increase in the background signal.

In Fig. 4a and 4b, we present results of a kinetic investigation of the process of FAM-ssDNA immobilization on both PANI and PPY films and show how the fluorescence intensity recovers as the hybridization of the FAM-ssDNA/ICP film system with its complementary DNA target proceeds. As it can be observed in Fig. 4a, for both types of films a 180 min of incubation time is required for the adsorption of the probe to reach equilibrium. When in presence of the complementary DNA target (Fig. 4b), a fast recovery of fluorescence occurs during the first 30 min, with the equilibrium situation being reached in 60 min. Thus, for both types of ICP/PET films the optimum times for the probe immobilization process and for the release of FAM-ssDNA were chosen as 180 min and 60 min, respectively.

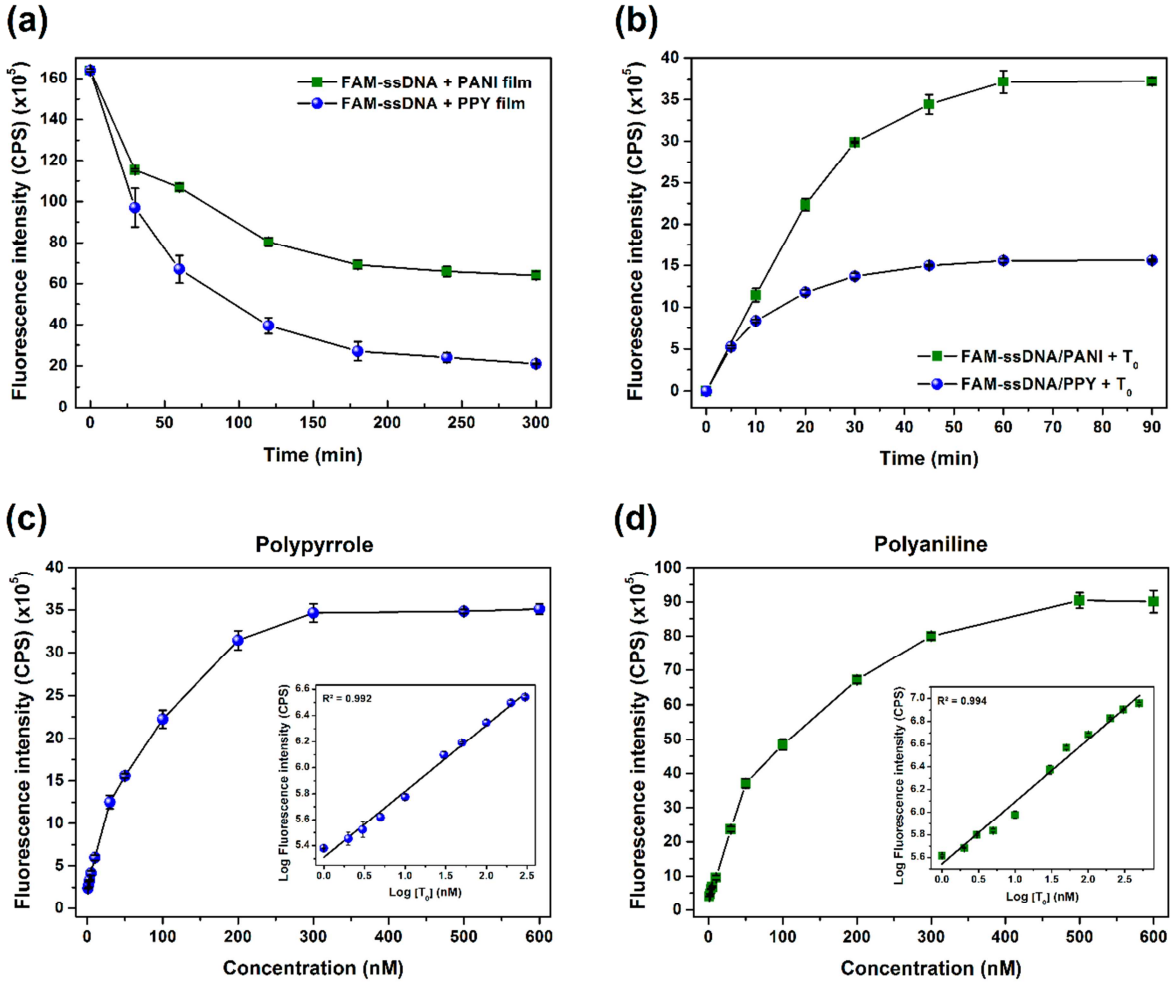

Figure 4. Kinetic study of (a) immobilization of FAM-ssDNA solution (75 nM) on PPY and PANI films and (b) fluorescence recovery of immobilized FAM-ssDNA after interaction of FAM-ssDNA/PPY and FAM-ssDNA/PANI systems with complementary target ssDNA (50 nM). Intensity of the fluorescence response of the (c) FAM-ssDNA/PPY and (d) FAM-ssDNA/PANI systems upon the addition of the complementary target ssDNA in the (1-600) nM range (the inset in the figures corresponds to the range of linear response of the assay).

3.4. Sensitivity of the *Leishmania infantum* DNA detection

To evaluate the range of sensing effectiveness as well as the lower detection limit for the PPY and PANI films, we implemented a detailed study employing different concentrations of the complementary DNA target. The recovery of fluorescence for T_0 in the 1 to 600 nM range for PPY and PANI is shown in Figs. 4c and 4d. As it can be seen, a larger amount of FAM-ssDNA is released from the surface of the films upon their exposure to increasing concentrations of the target

DNA; consequently, there is an increase in the measured fluorescence intensity due to the larger number of dsDNA chains formed. The saturation situation is reached at a concentration of 300 nM [500 nM] for the PPY [PANI] films. A linear relation with a coefficient of determination (R^2) equal to 0.994 was found between the fluorescence intensity at 520 nm (***F***) and the concentration of the target DNA (***C***), in the form log ***F*** = 0.548 log ***C*** + 5.54, in the (1–500) nM range, for the PANI films. For the PPY films, a high R^2 (0.992) was also obtained in the (1–300) nM range for the fitting log ***F*** = 0.508 log ***C*** + 5.31. The limit of detection was estimated as 1.1 nM [1.3 nM] for the PPY [PANI] films, by using the relation $3\sigma/S$ (where σ = standard deviation of the blank sample, and S the slope of the calibration curve) [49].

In Table 2, we show that the performance of the FAM-ssDNA/ICP films compares favorably to other sensing systems discussed in the literature, both in terms of the limit of detection and the range for DNA quantification. It is also important to note that since our active sensing material is in the form of films, a simple manipulation and retrieval becomes possible; with this, any non-immobilized probes can be discarded with the supernatant, reducing the background signal of the sample to be analyzed. In addition, agglomeration of the adsorbent, which can become a limiting factor when some nanostructures are used, is much reduced when the active material is deposited in the form of films.

Table 2. Performance of the PPY and PANI films for nucleic acid detection compared to those of different nanostructures reported in the literature.

Platform/structure	**Analyzed range (nM)**	**Linear range (nM)**	**Detection limit (nM)**	**Refs.**
AgNCs/GO nanoclusters	0 – 200	10 – 100	1.18	[50]
Bamboo-like NCNTs nanotubes	5 – 300	–	5.0	[51]
Carbon nanobelts	5 – 300	–	5.0	[52]
cCQD quantum dots	0.04 – 400	0.04 – 400	17.4	[16]
Fe-NTA nanowires	0.2 – 300	0.2 – 20	0.2	[15]
MoS_2 nanosheet	0.5 – 50	0.5 – 15	0.5	[24]

MPC hexagonal rods	0 – 600	3 – 150	1.0	[53]
Oc-AgNPs spherical colloids	2.5 – 300	2.5 – 25	1.8	[11]
PANI nanofibers	2.5 – 1000	–	2.5	[28]
PPPD nanobelts	30 – 300	30 – 300	30.0	[54]
PPY nanospheres	1.0 – 300	–	1.0	[27]
UiO-66-NH_2 MOFs	10 – 150	–	10.0	[55]
PANI films	**1 – 600**	**1 – 500**	**1.3**	***This work***
PPY films	**1 – 600**	**1 – 300**	**1.1**	***This work***

AgNCs: silver nanoclusters; **GO**: graphene oxide; **NCNTs**: nitrogen-doped carbon nanotubes; **cCQD**: carboxylic carbon quantum dots; **NTA**: nitrilotriacetic acid; **MPC**: magnetic porous carbon; **Oc-AgNPs**: polysaccharide-capped silver nanoparticles; **PPPD**: poly(p-phenylenediamine); **UiO-66-NH_2 MOFs**: amine-functionalized metal–organic framework.

Another important characteristic of the ICP/PET films and the FAM-ssDNA/ICP film systems is that they can be stored for later use, as necessary. We have found that when stored under ambient conditions the ICP/PET films preserve their characteristics so that they can be later functionalized for use in fluorescence assays. In fact, during this work we have performed DNA sensing tests using films prepared weeks or months beforehand (some of the films tested were 180-day old). As for the functionalized films already containing the immobilized probe (FAM-ssDNA/ICP systems), the data shown in Fig. S7 confirm that, if maintained at low temperature (10 °C), the FAM-ssDNA/ICP films retain their fluorescence response when exposed to the complementary target DNA solution even after several days of storage.

These results indicate that the fluorescence detection system here proposed allows a simple quantitative assessment of the target DNA content and provides a new perspective for the application of nanostructured films in fluorescent biosensing fields. Also, the excellent stability exhibited by the ICP/PET films functionalized with the DNA probe of interest suggests that they can find application in point-of-care molecular diagnostic protocols as strip tests.

3.5. Selectivity towards the *Leishmania infantum* DNA detection

Sensitivity is a relevant characteristic to consider in the evaluation of a sensing system, but the selectivity towards specific target molecules is also an important performance parameter to be examined. To investigate the recovery of the fluorescence intensity of the FAM-ssDNA/ICP film systems, we used distinct types of target ssDNA: i) perfectly complementing ssDNA (T_0), ii) single (T_1) and iii) two-base mismatched (T_2), and iv) non-complementary ssDNA (ncDNA) (see Table 1) at a fixed concentration (50 nM). As shown in Fig. 5a, in the case of the PPY films the fluorescence recovery intensity for T_1 [T_2] was significantly smaller (32% [18%]) than the value obtained when the full complementary target ssDNA was used. In a similar manner, for the PANI films the corresponding values were 37% and 23% (Fig. 5b). In addition, almost no change in fluorescence was observed when either the FAM-ssDNA/PPY or FAM-ssDNA/PANI system was exposed to the non-complementary ssDNA target.

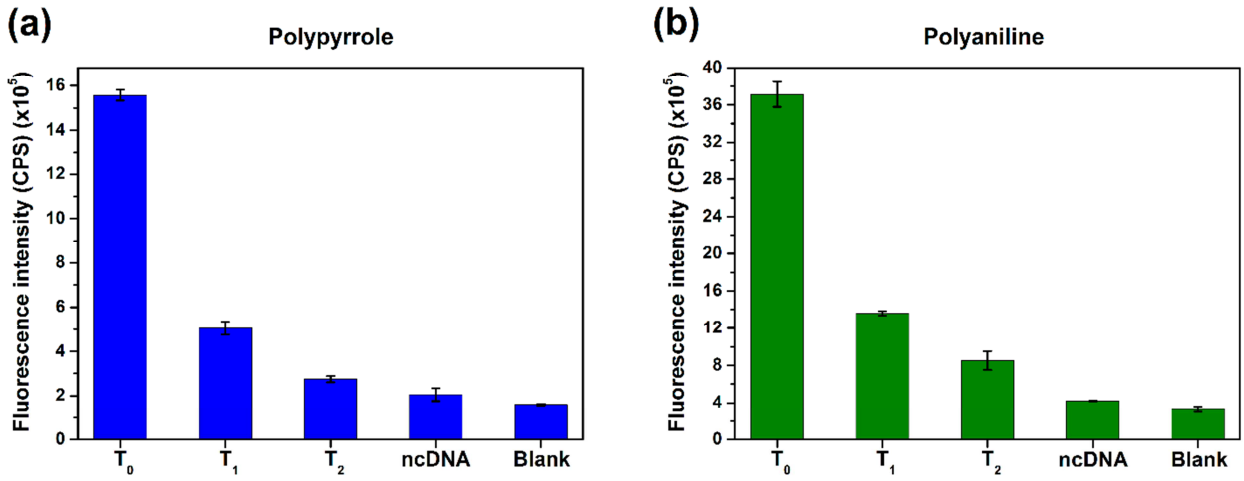

Figure 5. Histograms of the selectivity of the (a) FAM-ssDNA/PPY and (b) FAM-ssDNA/PANI systems towards the addition of (T_0) complementary, (T_1) one-base mismatched, (T_2) two-base-mismatched, and (ncDNA) non-complementary target ssDNA.

The fact that these results could be obtained with good reproducibility are suggestive that the observed increase in the fluorescence intensity result from the pairing of the complementary bases of the immobilized probe with the appropriate targets. Both types of detection systems present

a high selectivity towards the correct target DNA, as demonstrated by the smaller response observed even when oligonucleotide sequences with just a single base mismatch were tested.

3.6. Analysis in more complex media

For evaluating the potential of application of this novel sensing system in analyzing more realistic samples, we tested its performance in the assessment of the complementary ssDNA content in human blood serum (HBS) samples. For this, pretreated HBS samples (see Supporting Information) and 10x-diluted in Tris-HCl buffer (pH 7.4, in presence of 10 mM $MgCl_2$) were spiked with different concentrations (1, 5, 10, 20, 30 and 50 nM) of the target ssDNA by the standard addition method. Afterwards, these analyte solutions were examined using the FAM-ssDNA/ICP film systems. After constructing a new calibration curve (Fig. 6), we verified that for both ICP systems evaluated a good linear relationship exists between the fluorescence intensity and the target ssDNA concentration in HBS samples (the correlation coefficient R^2 is 0.99 and 0.98 for PPY and PANI, respectively). The corresponding relative standard deviations (RSD, n = 5) are all smaller than 5%.

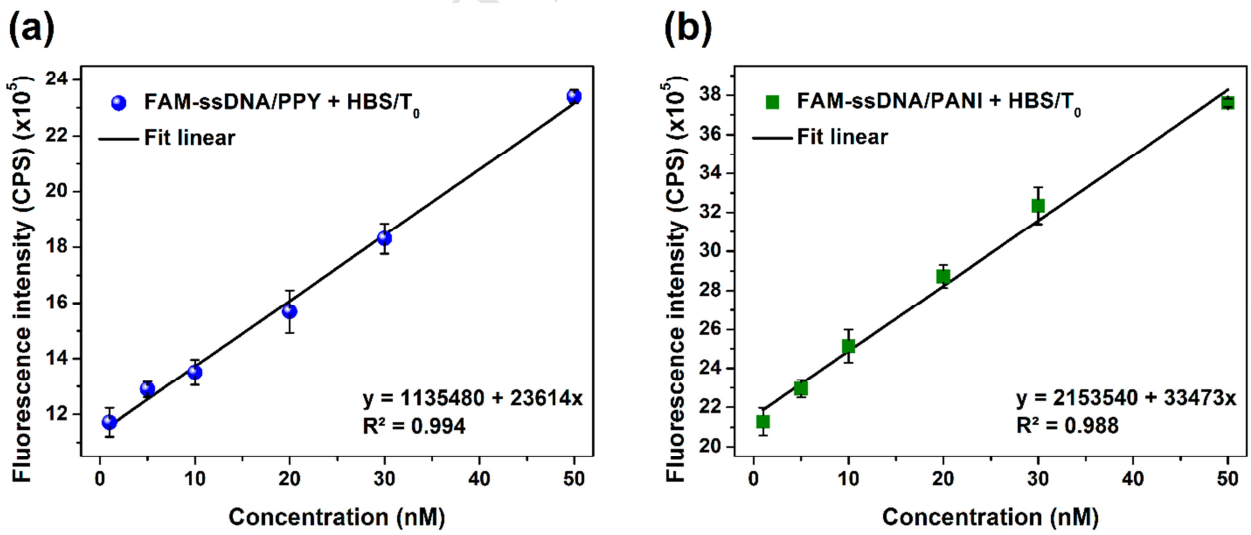

Figure 6. Calibration curves for the fluorescence response of the (a) FAM-ssDNA/PPY and (b) FAM-ssDNA/PANI systems. In both cases, the variation of the fluorescence intensity is linear with the increase in concentration of the complementary target ssDNA in 10x-diluted HBS samples.

These results are indicative that the biosensor based in FAM-ssDNA/ICP film systems can be used for the direct detection of nucleic acid content in relatively complex biological media and has the potential for future application in tests using real samples. However, several hurdles have to be faced before a direct application of this technology for the analysis of actual patient samples is attained. An example of this is the definition of the most practical protocol for converting the dsDNA found in a complex biological matrix to the ssDNA required for using the sensor, a challenge that still remains open in the area.

4. CONCLUSION

In this work, PPY and PANI films deposited on PET foils in a simple and inexpensive manner were successfully employed as a novel sensitive fluorescent sensing platform for the selective detection of nucleic acids. Our results indicate that both types of polymeric films exhibit high sensitivity, with the respective detection limits estimated as 1.1 nM (PPY) and 1.3 nM (PANI). It was found that the intensity of the fluorescence response can be observed as linear when the concentration of the target DNA is varied in a relatively large range – (1–300) nM and (1–500) nM, for PPY and PANI, respectively.

The FAM-ssDNA/ICP sensors present high selectivity and can discriminate even between full complementary sequences and those with just a single-mismatch. In addition, they can be used for DNA detection in a complex medium such as human blood serum. Considering these characteristics and the fact that functionalized ICP films exhibit good shelf stability, we suggest that these nanostructured ICP films can find practical applications as strip tests for the fast and sensitive fluorescent DNA detection in point-of-care clinical diagnosis protocols.

ACKNOWLEDGMENT

This work was supported by the Brazilian agencies CNPq, FACEPE and ELINOR Nanobiotechnology network. GCP, FDSG, RJS and KTON are grateful for CNPq and CAPES scholarships. JCML and AECG acknowledge financial support from the Mexican agency CONACyT. The authors would like to thank the Analytic Center of the Universidade Federal do Ceará, and the technical staffs of the UFPE Physics Department and CETENE for the SEM and AFM micrographs.

CONFLICTS OF INTEREST

The authors declare no competing financial interest.

APPENDIX A. SUPPLEMENTARY DATA

Supplementary data

REFERENCES

1. Sassolas, A., B.D. Leca-Bouvier, and L.J. Blum, *DNA Biosensors and Microarrays.* Chem. Rev., 2008. **108**(1): p. 109-139.
2. Wei, F., P.B. Lillehoj, and C.M. Ho, *DNA diagnostics: nanotechnology-enhanced electrochemical detection of nucleic acids.* Pediatr. Res., 2010. **67**(5): p. 458-68.
3. Nelson, B.P., et al., *Surface Plasmon Resonance Imaging Measurements of DNA and RNA Hybridization Adsorption onto DNA Microarrays.* Anal. Chem., 2001. **73**(1): p. 1-7.
4. Long, F., et al., *Rapid on-site/in-situ detection of heavy metal ions in environmental water using a structure-switching DNA optical biosensor.* Sci. Rep., 2013. **3**: p. 2308.
5. Lazerges, M. and F. Bedioui, *Analysis of the evolution of the detection limits of electrochemical DNA biosensors.* Anal. Bioanal. Chem., 2013. **405**(11): p. 3705-3714.
6. Cagnin, S., et al., *Overview of Electrochemical DNA Biosensors: New Approaches to Detect the Expression of Life.* Sensors, 2009. **9**(4): p. 3122.
7. Riedel, M., et al., *Impedimetric DNA Detection—Steps Forward to Sensorial Application.* Anal. Chem., 2014. **86**(15): p. 7867-7874.
8. Park, J.-Y. and S.-M. Park, *DNA Hybridization Sensors Based on Electrochemical Impedance Spectroscopy as a Detection Tool.* Sensors, 2009. **9**(12): p. 9513.
9. Tost, J. and I.G. Gut, *Genotyping single nucleotide polymorphisms by MALDI mass spectrometry in clinical applications.* Clin. Biochem., 2005. **38**(4): p. 335-350.
10. Mao, X., et al., *A nanoparticle amplification based quartz crystal microbalance DNA sensor for detection of Escherichia coli O157:H7.* Biosens. Bioelectron., 2006. **21**(7): p. 1178-1185.
11. Yan, J.-K., et al., *Highly selective and sensitive nucleic acid detection based on polysaccharide-functionalized silver nanoparticles.* Spectrochim. Acta A, 2015. **134**: p. 17-21.
12. Liu, Z. and X. Su, *A novel fluorescent DNA sensor for ultrasensitive detection of Helicobacter pylori.* Biosens. Bioelectron., 2017. **87**: p. 66-72.

13. Tang, G., et al., *Luminescent lanthanide coordination polymer as a platform for DNA colorimetric detection.* Sens. Actuators B Chem., 2017. **244**: p. 571-576.

14. Liu, B., et al., *Mechanisms of DNA Sensing on Graphene Oxide.* Anal. Chem., 2013. **85**(16): p. 7987-7993.

15. Yunchun, Z., et al., *Fe-nitrilotriacetic acid coordination polymer nanowires: an effective sensing platform for fluorescence-enhanced nucleic acid detection.* Nanotechnology, 2017. **28**(7): p. 075101.

16. Loo, A.H., et al., *Carboxylic Carbon Quantum Dots as a Fluorescent Sensing Platform for DNA Detection.* ACS Appl. Mater. Interfaces, 2016. **8**(3): p. 1951-1957.

17. Qiang, W., et al., *Bioinspired polydopamine nanospheres: a superquencher for fluorescence sensing of biomolecules.* Chem. Sci., 2014. **5**(8): p. 3018-3024.

18. He, S., et al., *A Graphene Nanoprobe for Rapid, Sensitive, and Multicolor Fluorescent DNA Analysis.* Adv. Funct. Mater., 2010. **20**(3): p. 453-459.

19. Yang, R., et al., *Noncovalent Assembly of Carbon Nanotubes and Single-Stranded DNA: An Effective Sensing Platform for Probing Biomolecular Interactions.* Anal. Chem., 2008. **80**(19): p. 7408-7413.

20. Dubertret, B., M. Calame, and A.J. Libchaber, *Single-mismatch detection using gold-quenched fluorescent oligonucleotides.* Nat. Biotechnol., 2001. **19**(4): p. 365-370.

21. Zhang, Y.-W., H.-L. Li, and X.-P. Sun, *Silver Nanoparticles as a Fluorescent Sensing Platform for Nucleic Acid Detection.* Chinese J. Anal. Chem., 2011. **39**(7): p. 998-1002.

22. Bülbül, G., et al., *DNA assay based on Nanoceria as Fluorescence Quenchers (NanoCeracQ DNA assay).* Scientific Reports, 2018. **8**(1): p. 2426.

23. Zhao, H.-Q., et al., *A zinc(II)-based two-dimensional MOF for sensitive and selective sensing of HIV-1 ds-DNA sequences.* Anal. Chim. Acta, 2016. **922**: p. 55-63.

24. Zhu, C., et al., *Single-Layer MoS2-Based Nanoprobes for Homogeneous Detection of Biomolecules.* J. Am. Chem. Soc., 2013. **135**(16): p. 5998-6001.

25. Mo, L., et al., *Nucleic acid-functionalized transition metal nanosheets for biosensing applications.* Biosens. Bioelectron., 2017. **89, Part 1**: p. 201-211.

26. Zhang, Y., et al., *Novel Use of Poly(3,4-ethylenedioxythiophene) Nanoparticles for Fluorescent Nucleic Acid Detection.* ACS Comb. Sci., 2012. **14**(3): p. 191-196.

27. Lu, W., et al., *Polypyrrole colloidal nanospheres as an effective fluorescent sensing platform for DNA detection.* Synthetic Met., 2011. **161**(15): p. 1766-1770.

28. Liu, S., et al., *Polyaniline nanofibres for fluorescent nucleic acid detection.* Nanoscale, 2011. **3**(3): p. 967-969.

29. Wang, S., et al., *Flexible Substrate-Based Devices for Point-of-Care Diagnostics.* Trends in Biotechnology, 2016. **34**(11): p. 909-921.

30. Li, D., J. Huang, and R.B. Kaner, *Polyaniline Nanofibers: A Unique Polymer Nanostructure for Versatile Applications.* Accounts Chem. Res., 2009. **42**(1): p. 135-145.

31. Zhang, X. and Bai, *Surface Electric Properties of Polypyrrole in Aqueous Solutions.* Langmuir, 2003. **19**(26): p. 10703-10709.

32. Medina-Llamas, J.C., et al., *Use of magnetic polyaniline/maghemite nanocomposite for DNA retrieval from aqueous solutions.* J. Colloid. Interf. Sci., 2014. **434**: p. 167-174.

33. Strain, I.N., et al., *Electrospinning of recycled PET to generate tough mesomorphic fibre membranes for smoke filtration.* J. Mater. Chem. A, 2015. **3**(4): p. 1632-1640.

34. Guo, Z., et al., *Fabrication and characterization of iron oxide nanoparticles filled polypyrrole nanocomposites.* J. Nanopart. Res., 2009. **11**(6): p. 1441-1452.

35. Zhang, H., et al., *Fe3O4/Polypyrrole/Au Nanocomposites with Core/Shell/Shell Structure: Synthesis, Characterization, and Their Electrochemical Properties.* Langmuir, 2008. **24**(23): p. 13748-13752.

36. Chávez-Guajardo, A.E., et al., *Efficient removal of Cr (VI) and Cu (II) ions from aqueous media by use of polypyrrole/maghemite and polyaniline/maghemite magnetic nanocomposites.* Chem. Eng. J., 2015. **281**(Supplement C): p. 826-836.

37. Jiang, J., L. Li, and M. Zhu, *Polyaniline/magnetic ferrite nanocomposites obtained by in situ polymerization.* React. Funct. Polym., 2008. **68**(1): p. 57-62.

38. Alcaraz-Espinoza, J.J., et al., *Hierarchical Composite Polyaniline–(Electrospun Polystyrene) Fibers Applied to Heavy Metal Remediation.* ACS Appl. Mater. Interfaces, 2015. **7**(13): p. 7231-7240.

39. Reung-U-Rai, A., et al., *Synthesis of highly conductive polypyrrole nanoparticles via microemulsion polymerization.* Journal of Metals, Materials and Minerals, 2008. **18**(2): p. 27-31.

40. Jang, K.S., H. Lee, and B. Moon, *Synthesis and characterization of water soluble polypyrrole doped with functional dopants.* Synthetic Metals, 2004. **143**(3): p. 289-294.

41. Stejskal, J., P. Kratochvíl, and N. Radhakrishnan, *Polyaniline dispersions 2. UV—Vis absorption spectra.* Synthetic Metals, 1993. **61**(3): p. 225-231.

42. Gorza, F.D.S., et al., *Electrospun polystyrene-(emeraldine base) mats as high-performance materials for dye removal from aqueous media.* J. Taiwan Inst. Chem. E., 2018. **82**: p. 300-311.

43. Chiou, N.-R., et al., *Growth and alignment of polyaniline nanofibres with superhydrophobic, superhydrophilic and other properties.* Nat. Nanotech., 2007. **2**(6): p. 354-357.

44. Stejskal, J. and I. Sapurina, *Polyaniline: Thin films and colloidal dispersions (IUPAC Technical Report).* Pure Appl. Chem., 2005. **77**(5): p. 815-826.

45. Liu, J., et al., *Templateless Assembly of Molecularly Aligned Conductive Polymer Nanowires: A New Approach for Oriented Nanostructures.* Chemistry – A European Journal, 2003. **9**(3): p. 604-611.

46. Ferenets, M. and A. Harlin, *Chemical in situ polymerization of polypyrrole on poly(methyl metacrylate) substrate.* Thin Solid Films, 2007. **515**(13): p. 5324-5328.

47. Malinauskas, A., *Chemical deposition of conducting polymers.* Polymer, 2001. **42**(9): p. 3957-3972.

48. Nakao, H., et al., *Development of Novel Polymer-Coated Substrates for Straightening and Fixing DNA.* Nano Lett., 2002. **2**(5): p. 475-479.

49. Ye, Y.-D., et al., *DNA-stabilized silver nanoclusters and carbon nanoparticles oxide: A sensitive platform for label-free fluorescence turn-on detection of HIV-DNA sequences.* Biosens. Bioelectron., 2016. **85**(Supplement C): p. 837-843.

50. Zhang, S., et al., *A DNA-stabilized silver nanoclusters/graphene oxide-based platform for the sensitive detection of DNA through hybridization chain reaction.* Biosens. Bioelectron., 2017. **91**: p. 374-379.

51. Liu, Q., et al., *Bamboo-like nitrogen-doped carbon nanotubes toward fluorescence recovery assay for DNA detection.* Sens. Actuators B Chem., 2015. **206**(Supplement C): p. 37-42.

52. Sun, X., et al., *Carbon nanobelts as a novel sensing platform for fluorescence-enhanced DNA detection.* Analyst, 2014. **139**(10): p. 2318-2321.

53. Tan, H., et al., *Magnetic porous carbon nanocomposites derived from metal-organic frameworks as a sensing platform for DNA fluorescent detection.* Anal. Chim. Acta, 2016. **940**(Supplement C): p. 136-142.

54. Wang, L., et al., *Conjugation polymer nanobelts: a novel fluorescent sensing platform for nucleic acid detection.* Nucleic Acids Res., 2011. **39**(6): p. e37-e37.

55. Zhang, H.-T., et al., *An amine-functionalized metal-organic framework as a sensing platform for DNA detection.* Chem. Commun., 2014. **50**(81): p. 12069-12072.

A novel nucleic acid fluorescent sensing platform based on nanostructured films of intrinsically conducting polymers

Graciela C. Pedro [a], Filipe D. S. Gorza [a], Romário J. da Silva [a], Kamila T. O. do Nascimento [a],
Juan C. Medina-Llamas [b], Alicia E. Chávez-Guajardo [c], José J. Alcaraz-Espinoza [d],
Celso P. de Melo [a, d *]

[a] *Pós-Graduação em Ciência de Materiais, Universidade Federal de Pernambuco, 50670-901 Recife, PE, Brazil*

[b] *Centro de Estudios Científicos y Tecnológicos No. 18, Instituto Politécnico Nacional, 98160, Zacatecas, Zac, Mexico*

[c] *Unidad Académica de Ciencias de la Tierra, Universidad Autónoma de Zacatecas, 98058 Zacatecas, Zac, Mexico*

[d] *Departamento de Física, Universidade Federal de Pernambuco, 50670-901 Recife, PE, Brazil*

Table 1. Oligonucleotide sequences used in this work (mismatch underlined).

Name	Oligonucleotide sequence
FAM-ssDNA Linf.1-23F – *Leishmania*	5'- FAM-TCC CAA ACT TTT CTG GTC CT -3'
Complementary target DNA (T_0)	5'- AGG ACC AGA AAA GTT TGG GA -3'
Single-base-mismatched target DNA (T_1)	5'- AGG ACC AGA **C**AA GTT TGG GA -3'
Two-base-mismatched target DNA (T_2)	5'- AGG ACC AGA **C**A**C** GTT TGG GA -3'
Non-complementary target DNA (ncDNA)	5'- GAA ACT GGG GGT TGG TGT AA -3'

A novel nucleic acid fluorescent sensing platform based on nanostructured films of intrinsically conducting polymers

Graciela C. Pedro [a], Filipe D. S. Gorza [a], Romário J. da Silva [a], Kamila T. O. do Nascimento [a],
Juan C. Medina-Llamas [b], Alicia E. Chávez-Guajardo [c], José J. Alcaraz-Espinoza [d],
Celso P. de Melo [a, d *]

[a] *Pós-Graduação em Ciência de Materiais, Universidade Federal de Pernambuco, 50670-901 Recife, PE, Brazil*

[b] *Centro de Estudios Científicos y Tecnológicos No. 18, Instituto Politécnico Nacional, 98160, Zacatecas, Zac, Mexico*

[c] *Unidad Académica de Ciencias de la Tierra, Universidad Autónoma de Zacatecas, 98058 Zacatecas, Zac, Mexico*

[d] *Departamento de Física, Universidade Federal de Pernambuco, 50670-901 Recife, PE, Brazil*

Table 2. Performance of the PPY and PANI films for nucleic acid detection compared to those of different nanostructures reported in the literature.

Platform/structure	Analyzed range (nM)	Linear range (nM)	Detection limit (nM)	Refs.
AgNCs/GO nanoclusters	0 – 200	10 – 100	1.18	[50]
Bamboo-like NCNTs nanotubes	5 – 300	–	5.0	[51]
Carbon nanobelts	5 – 300	–	5.0	[52]
cCQD quantum dots	0.04 – 400	0.04 – 400	17.4	[16]
Fe-NTA nanowires	0.2 – 300	0.2 – 20	0.2	[15]
MoS_2 nanosheet	0.5 – 50	0.5 – 15	0.5	[24]
MPC hexagonal rods	0 – 600	3 – 150	1.0	[53]
Oc-AgNPs spherical colloids	2.5 – 300	2.5 – 25	1.8	[11]
PANI nanofibers	2.5 – 1000	–	2.5	[28]
PPPD nanobelts	30 – 300	30 – 300	30.0	[54]
PPY nanospheres	1.0 – 300	–	1.0	[27]
UiO-66-NH_2 MOFs	10 – 150	–	10.0	[55]
PANI films	**1 – 600**	**1 – 500**	**1.3**	***This work***
PPY films	**1 – 600**	**1 – 300**	**1.1**	***This work***

AgNCs: silver nanoclusters; **GO**: graphene oxide; **NCNTs**: nitrogen-doped carbon nanotubes; **cCQD**: carboxylic carbon quantum dots; **NTA**: nitrilotriacetic acid; **MPC**: magnetic porous carbon; **Oc-AgNPs**: polysaccharide-capped silver nanoparticles; **PPPD**: poly(p-phenylenediamine); **UiO-66-NH_2 MOFs**: amine-functionalized metal–organic framework.

A novel nucleic acid fluorescent sensing platform based on nanostructured films of intrinsically conducting polymers

Graciela C. Pedro [a], Filipe D. S. Gorza [a], Romário J. da Silva [a], Kamila T. O. do Nascimento [a],

Juan C. Medina-Llamas [b], Alicia E. Chávez-Guajardo [c], José J. Alcaraz-Espinoza [d], Celso P. de Melo [a, d *]

[a] *Pós-Graduação em Ciência de Materiais, Universidade Federal de Pernambuco, 50670-901 Recife, PE, Brazil*

[b] *Centro de Estudios Científicos y Tecnológicos No. 18, Instituto Politécnico Nacional, 98160, Zacatecas, Zac, Mexico*

[c] *Unidad Académica de Ciencias de la Tierra, Universidad Autónoma de Zacatecas, 98058 Zacatecas, Zac, Mexico*

[d] *Departamento de Física, Universidade Federal de Pernambuco, 50670-901 Recife, PE, Brazil*

Table S1. Values of the average roughness measurements of the ICP/PET films.

Number of polymerization cycles	PANI films	PPY films
1	89.7 ± 9.7 nm	76.7 ± 3.7 nm
2	105.3 ± 12.6 nm	82.6 ± 8.6 nm
3	115.9 ± 17.1 nm	90.4 ± 13.6 nm

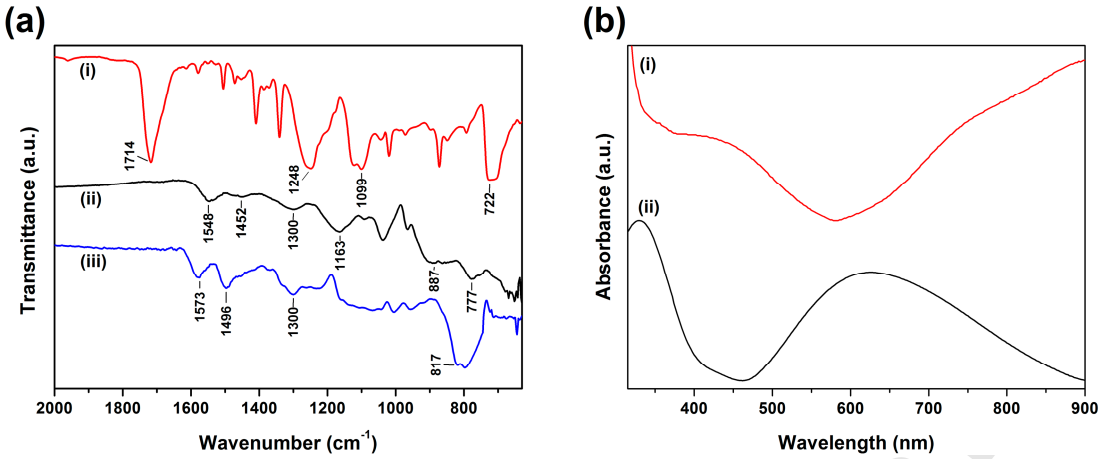

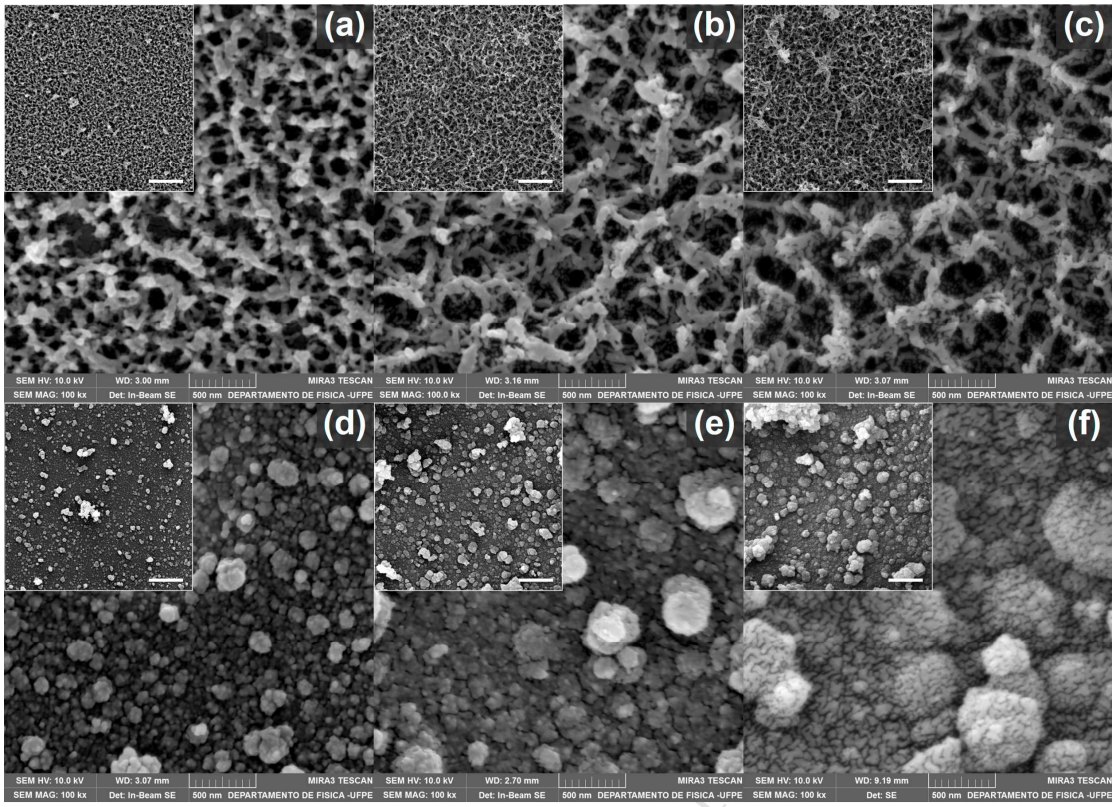

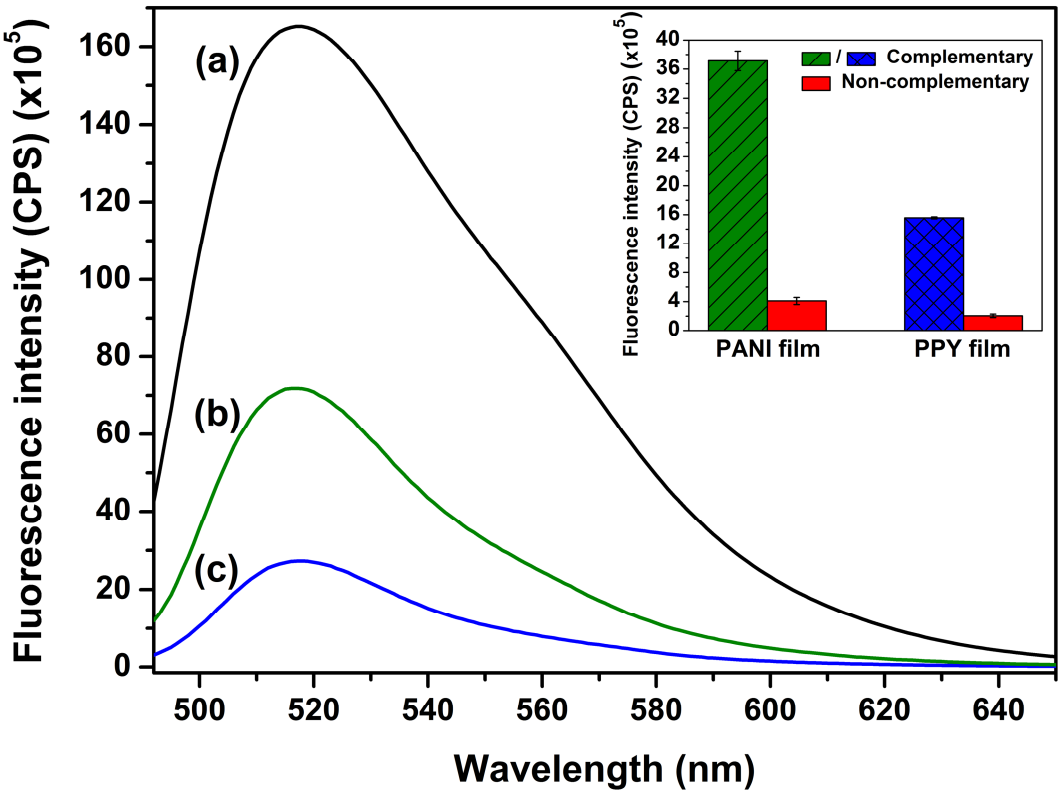

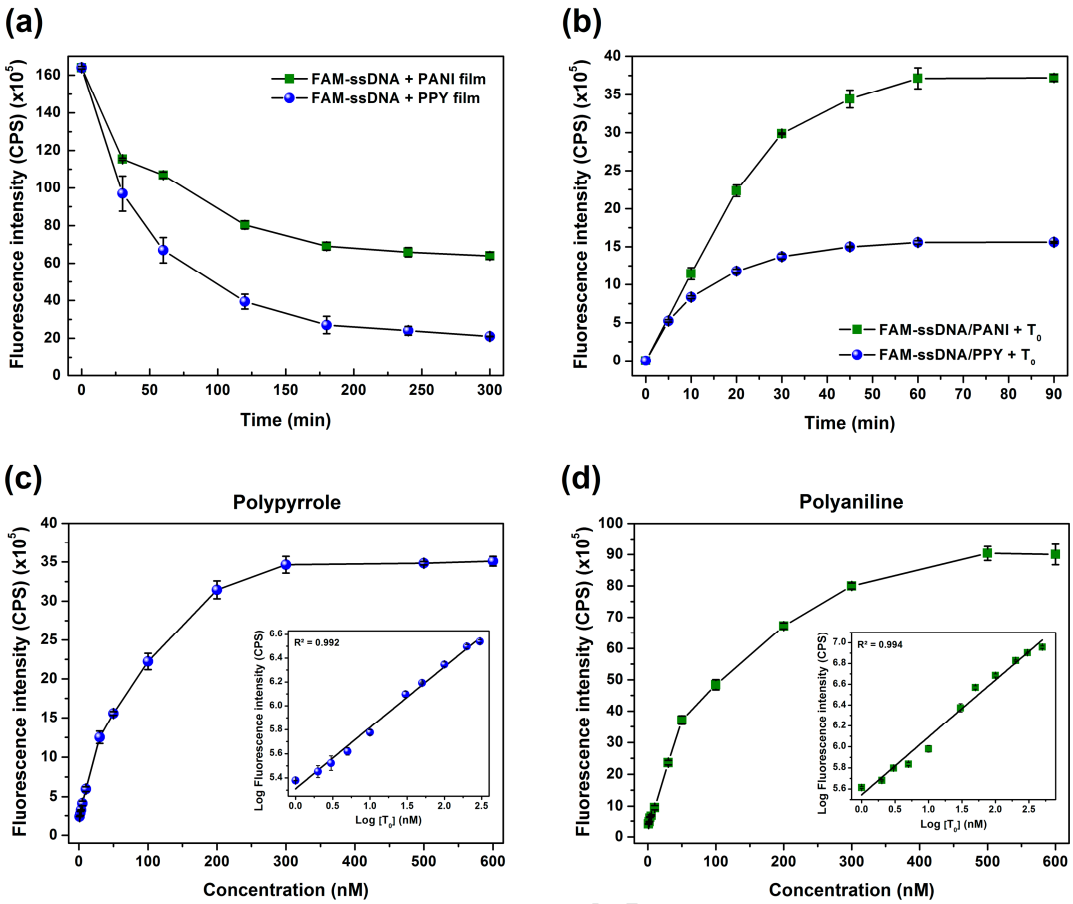

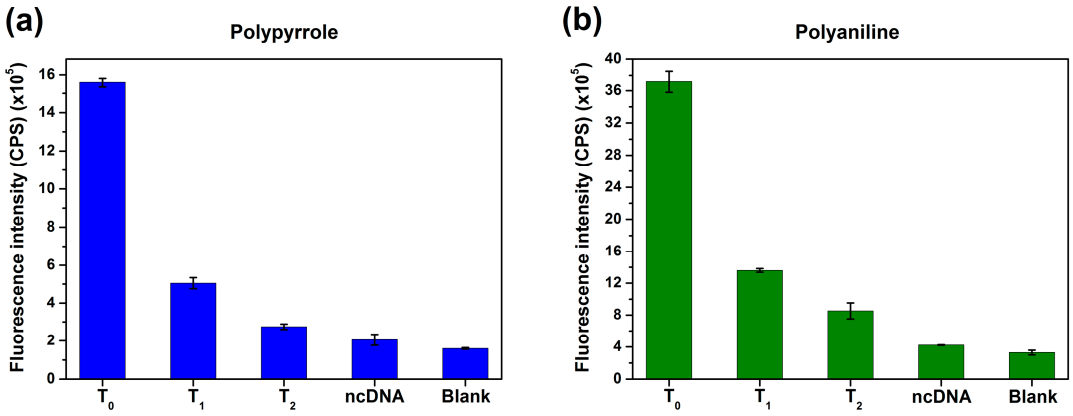

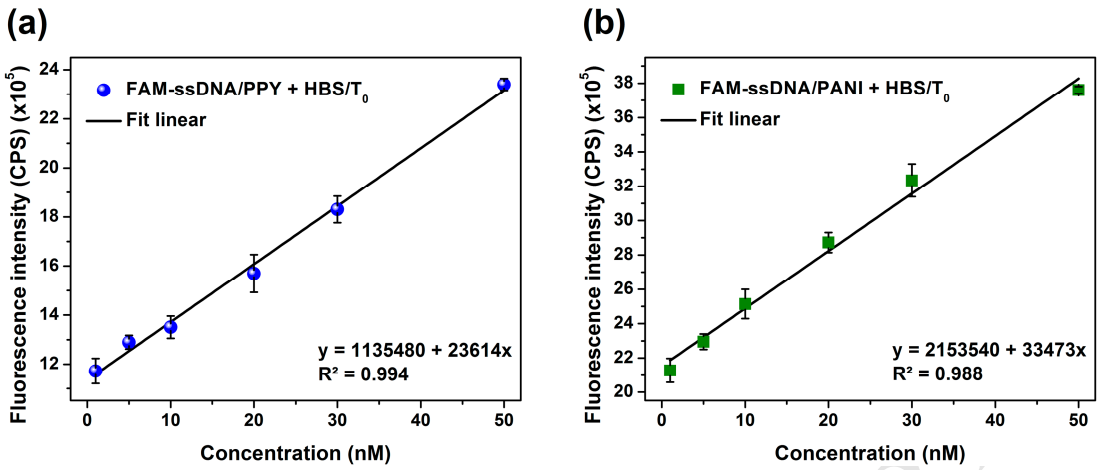

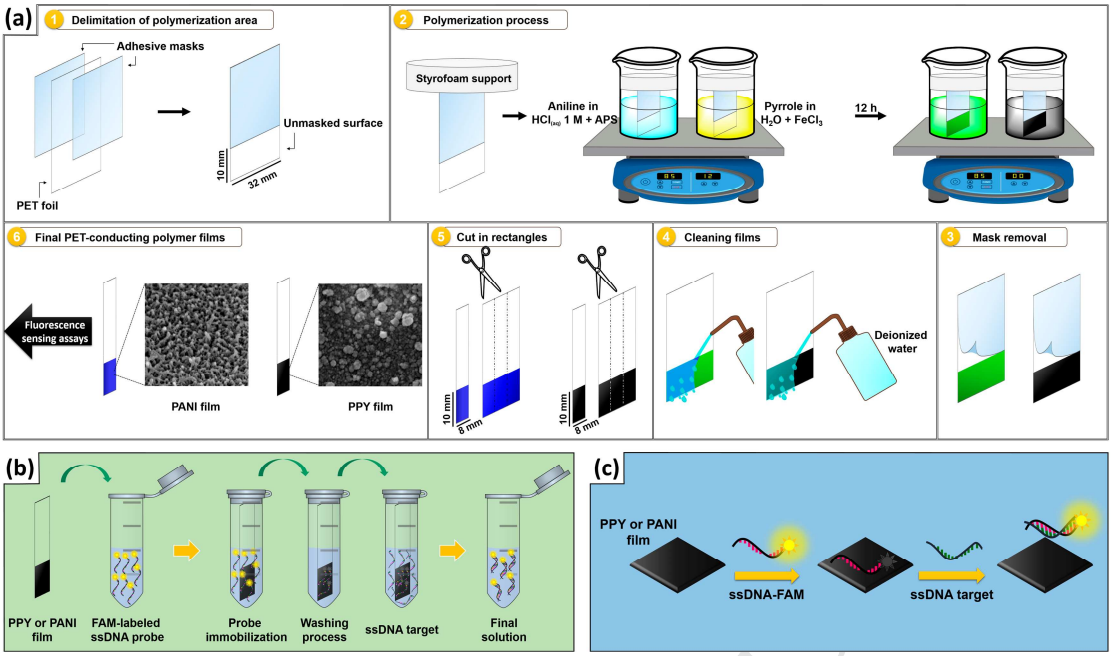

Highlights

- This is the first report on the use of conducting polymer-based films as fluorescence quenchers for DNA sensing
- The biosensor developed is highly sensitive and selective for detecting specific nucleic acid sequences
- These polymeric films are easy to handle and require simple and low-cost preparation procedures
- These polymeric films can be used in the convenient form of test strips
- This type of biosensor could be used as a universal DNA fluorescence detection platform